Journal of Biomedical Optics

SPIEDigitalLibrary.org/jbo

Transcutaneous *in vivo* Raman spectroscopic studies in a mouse model: evaluation of changes in the breast associated with pregnancy and lactation

Tanmoy Bhattacharjee
Girish Maru
Arvind Ingle
C. Murali Krishna

SPIE

Transcutaneous *in vivo* Raman spectroscopic studies in a mouse model: evaluation of changes in the breast associated with pregnancy and lactation

Tanmoy Bhattacharjee,[a] Girish Maru,[b] Arvind Ingle,[c] and C. Murali Krishna[a]
[a]Advanced Center for Treatment Research and Education in Cancer, Chilakapati Laboratory, Kharghar, Navi Mumbai 410210, India
[b]Advanced Center for Treatment Research and Education in Cancer, Maru Laboratory, Kharghar, Navi Mumbai 410210, India
[c]Advanced Center for Treatment Research and Education in Cancer, Laboratory Animal Facility, Kharghar, Navi Mumbai 410210, India

Abstract. Raman spectroscopy (RS) has been extensively explored as an alternative diagnostic tool for breast cancer. This can be attributed to its sensitivity to malignancy-associated biochemical changes. However, biochemical changes due to nonmalignant conditions like benign lesions, inflammatory diseases, aging, menstrual cycle, pregnancy, and lactation may act as confounding factors in diagnosis of breast cancer. Therefore, in this study, the efficacy of RS to classify pregnancy and lactation-associated changes as well as its effect on breast tumor diagnosis was evaluated. Since such studies are difficult in human subjects, a mouse model was used. Spectra were recorded transcutaneously from the breast region of six Swiss bare mice postmating, during pregnancy, and during lactation. Data were analyzed using multivariate statistical tool Principal Component–Linear Discriminant Analysis. Results suggest that RS can differentiate breasts of pregnant/lactating mice from those of normal mice, the classification efficiencies being 100%, 60%, and 88% for normal, pregnant, and lactating mice, respectively. Frank breast tumors could be classified with 97.5% efficiency, suggesting that these physiological changes do not affect the ability of RS to detect breast tumors. [DOI: 10.1117/1.JBO.18.4.047004]

Keywords: pregnancy; lactation; transcutaneous; *in vivo*; Raman spectroscopy.

Paper 12712R received Nov. 3, 2012; revised manuscript received Feb. 5, 2013; accepted for publication Mar. 19, 2013; published online Apr. 15, 2013.

1 Introduction

Breast cancer is the most frequently diagnosed cancer and the leading cause of cancer death in females worldwide, accounting for 23% (1.38 million) of the total new cancer cases and 14% (458,400) of the total cancer deaths in 2008.[1] Literature suggests improved prognosis with early detection of breast cancer.[2] However, currently available screening/diagnostic tools suffer from several disadvantages like tedious sample preparation, long output times, and interobserver variance.[3,4] Rapid, objective, and preferably noninvasive alternate screening/diagnostic techniques are hence being extensively explored. Raman spectroscopy (RS) is one such tool, which has shown promising results in the diagnosis of several cancers,[5] including breast cancers.[6,7] RS is an inelastic scattering process where the energy of photon scattered by the sample is different from the incident photon due to transfer of energy to or from vibrational modes of molecules in the sample.[8] Since bands of Raman spectrum are characteristic of specific molecular vibrations unique to a molecule, RS can provide the chemical fingerprint of a sample. However, biochemical changes also occur due to physiological processes like aging, menstrual cycle, pregnancy, and lactation.

Continuous changes take place in the breast as age progresses and the mice undergo different reproductive phases. During pregnancy and lactation, massive tissue remodeling occurs in the breast,[9] emphasizing the need to study these processes spectroscopically. At birth, the mammary glands consist of stroma-connective tissue, fibroblasts, the mammary fat pad, and epithelial cords which is a small, branched ductal network of mammary epithelium that invades from nipple into fat pad.[10] During puberty, the epithelium forms terminal end buds, which invade the fat pad resulting in branched ducts throughout the breasts. The final developmental stages of the mammary glands occur during pregnancy and lactation. Massive proliferation of ductal cells and alveolar buds takes place. The epithelial to adipocyte ratio increases and capillaries are found within the connective tissue surrounding each individual alveolus. During the second half of pregnancy, the alveolar buds progressively cleave and differentiate into individual alveoli that will ultimately transform into milk-secreting lobules during lactation. The mammary glands display many of the properties associated with tumor progression during pregnancy and lactation. For example, rapid proliferation of epithelial cells takes place during these phases. The lactating mammary gland also actively resists apoptotic signals.[11] In addition, as the mammary gland undergoes these morphological changes, its blood supply gets adjusted, and thus, like tumors, the mammary gland induces angiogenic remodeling.[12] Thus, changes in the breast during pregnancy and lactation have steps similar to carcinogenesis. Therefore, the potential of RS to detect malignant changes in light of these confounding factors needs to be evaluated. The ability of RS to differentiate benign lesions from normal and malignant conditions has been demonstrated.[6,7] The effect of aging on breast cancer diagnosis has also been explored.[6]

Address all correspondence to: C. Murali Krishna, Advanced Center for Treatment Research and Education in Cancer, Tata Memorial Center, Chilakapati Laboratory, Sector 22, Kharghar, Navi Mumbai 410210, India. Tel: +91-22-27405039; Fax: 91-22-2740 5085; E-mail: pittu1043@gmail.com or mchilakapati@actrec.gov.in

0091-3286/2013/$25.00 © 2013 SPIE

However, sensitivity of RS to other physiological changes (menstrual cycle, pregnancy, lactation) is yet to be ascertained.

The current study aims to evaluate the sensitivity of transcutaneous *in vivo* RS to changes in breasts of nonpregnant, pregnant, and lactating mice and its effect on breast tumor detection. In the study, spectra were recorded transcutaneously from breast of nonpregnant (control), pregnant, and lactating mice. To test the ability of this technique to differentiate between malignancy and pregnancy- or lactation-associated changes, transcutaneous spectra were also recorded from subcutaneously transplanted frank breast tumors. Data were analyzed using multivariate statistical tools. The findings of the study are discussed in the paper.

2 Materials and Methods

2.1 *Animals*

Female Swiss bare mice,[13] a hairless version of Swiss albino mice, were allowed to mate, and successful mating was identified by appearance of vaginal plugs. Successful pregnancy was determined by observation of visible bulge in the abdominal region of mice (approximately 2 weeks postmating). Delivery of pups marked the beginning of the lactation phase (approximately 3 weeks postmating). These different stages were established by a veterinarian. To minimize variability in data, the same set of mice were used to record spectra immediately postmating, during pregnancy (2 weeks postmating), and lactation (1 to 2 days postdelivery). Between 8 and 11 spectra per mouse were recorded transcutaneously from left and right inguinal breast of mice, resulting in 56 to 60 spectra per group. Each spectrum was recorded approximately 1 mm apart by using a precision stage. Only spectra from mice ($n = 6$) who delivered live pups were used for analysis. The study was approved by Institutional Animal Ethics Committee. All animals were housed under standard laboratory conditions, fed a diet of in-house-prepared pellets, and provided with water *ad libitum*. The protocol employed in the study has been depicted in Fig. 1.

2.2 *Tumor Transplantation*

To record tumor spectra, tumors from the well-known mouse mammary tumor virus-induced spontaneous tumorogenesis model Indian Cancer Research Center mice were[14] extracted, cut into small pieces using a scalpel, washed in normal saline, and grafted (two tumors per mice) subcutaneously in the inguinal breast mammary fat pad region of the Swiss bare mice. Subcutaneous transplantation mimics the *in situ* location of breast tumors. The incisions made for transplantation were well away from the site of transplantation. This ensures that incisions in the skin do not influence the spectroscopic readings. Ten spectra were then recorded transcutaneously from four tumors transplanted in mice ($n = 2$) a day after surgery, resulting in a total of 40 spectra in the tumor group.

2.3 *Raman Spectroscopy*

All spectra were recorded using HE-785 (Jobin-Yvon-Horiba, France) Raman spectrometer described elsewhere.[15] Briefly, this system consists of a diode laser (Process Instruments) of 785 nm wavelength as excitation source, a high efficiency spectrograph with fixed 950 gr/mm grating coupled with a charge-coupled device (CCD) (Synapse). The spectrograph has no movable parts and the resolution is ~4 cm^{-1}. A commercially available (InPhotonics Inc., Downy St., USA) probe consisting of a 105 μm excitation fiber and a 200 μm collection fiber (numerical aperture = 0.40) was used to couple excitation source and detection system. The estimated spot size and depth of field as per the manufacturer's specifications is 105 μm and 1 mm, respectively. Spectral acquisition parameters were λex 785 nm, laser power 80 mW, spectra were integrated for 15 s and averaged over three accumulations.

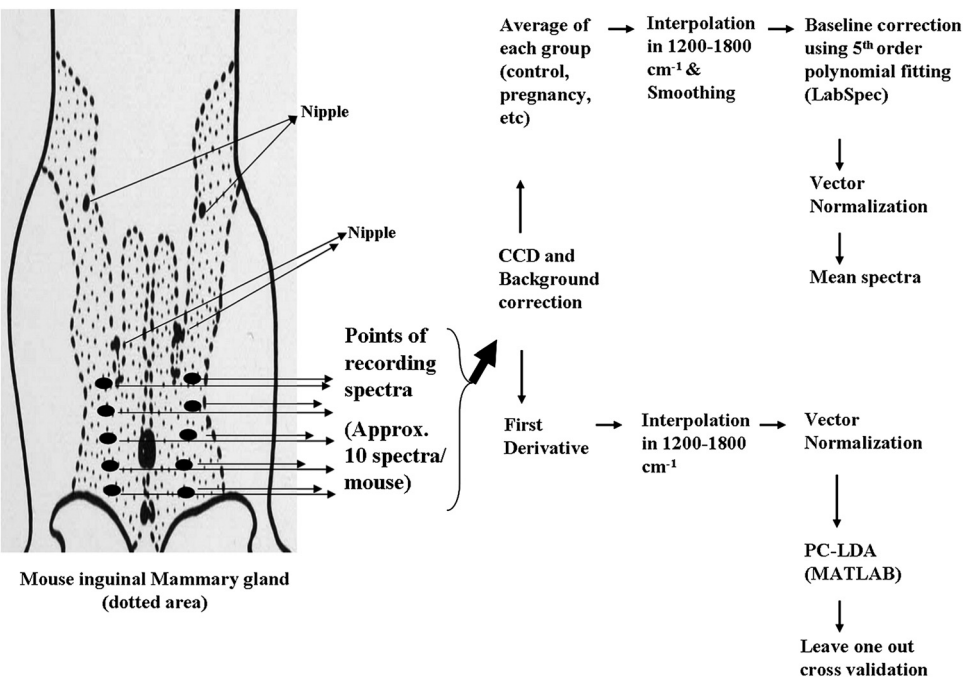

Fig. 1 Schematic representation of spectra acquisition, data preprocessing, and multivariate classification protocols.

2.4 *Data Analysis*

The protocol for data analysis[16–18] is as follows. Spectra recorded from mouse breasts of different groups were preprocessed by correcting for CCD response with a National Institute of Standards and Technology certified SRM 2241 material and subtraction of background signals from optical elements. To remove interference of the slow-moving background, first derivative of the preprocessed Raman spectra was calculated (Savitzky-Golay, window size 3), interpolated in the 1200 to 1800 cm^{-1} range (Raman fingerprint region), and vector normalized. Classification of different groups was achieved using the multivariate analysis tool Principal Component–Linear Discriminant Analysis (PC-LDA)[19,20] implemented in MATLAB (Mathwork Inc.) based in-house software.[21]

First derivatives of preprocessed spectra were subjected to supervised PC-LDA. PCA is the routinely used method for data compression and visualization. It describes data variance by identifying a new set of orthogonal features, which are called principal components (PCs) that are linear combinations of original data variables. These PCs are calculated by identifying eigenvectors for the covariance matrix of mean-centered data. Because of their orthogonal characteristics, first few PCs are enough to represent maximum data variance. And for visual discrimination, we project each of the spectra in the newly formed coordinate space of these selected PCs. While PCA aims to identify features that represent variance among complete data, LDA provides data classification based on an optimized criterion which is aimed for more class separability. LDA is a method of choice when input data have higher within-class variance that could lead to development of PCs that are inappropriate for visual discrimination. The classification criterion is identified using the scatter measure of within-class and between-class variances. LDA transformations are further identified as eigenvector matrix of this classification criterion. With the help of this LDA transform matrix, any test spectra can be classified to a class by iteratively calculating Euclidean/Root Mean Square or Mahalanobis distance of transformed test spectra and the mean of transformed input data set. In this study, we have employed Mahalanobis distance for class prediction, since it handles nonlinearity well.[22] LDA can be used in companion with PCA (PC-LDA) to further increase the performance efficiency of classification. For this, PCA scores obtained using a set of few PCs with maximum variance amongst data are used as input data for LDA-based classification. The advantage of doing this is to remove or minimize noise from the data and concentrate on variables important for classification. In our analysis, PC-LDA models were further validated by leave-one-out cross-validation (LOOCV).

The results of PC-LDA are depicted in the form of a confusion matrix, where all diagonal elements are true positive predictions and ex-diagonal elements are false positive predictions. The confusion matrix is generated to understand the separation between the groups obtained by taking into account contribution of all factors selected for analysis. These results can also be depicted in the form of scatter plots generated by plotting combinations of scores of factors. Plotting different combinations of factor scores give a visual understanding of classification patterns in the data.

Average spectra were computed from the background subtracted spectra (without derivatization) for each class and baseline corrected by fitting a fifth-order polynomial function. The spectra were smoothed postaveraging using LabSpec 4.18 (average method, window size 3), for representing the mean spectra (Fig. 2). These baseline-corrected, vector-normalized spectra were used for spectral comparisons and for computing

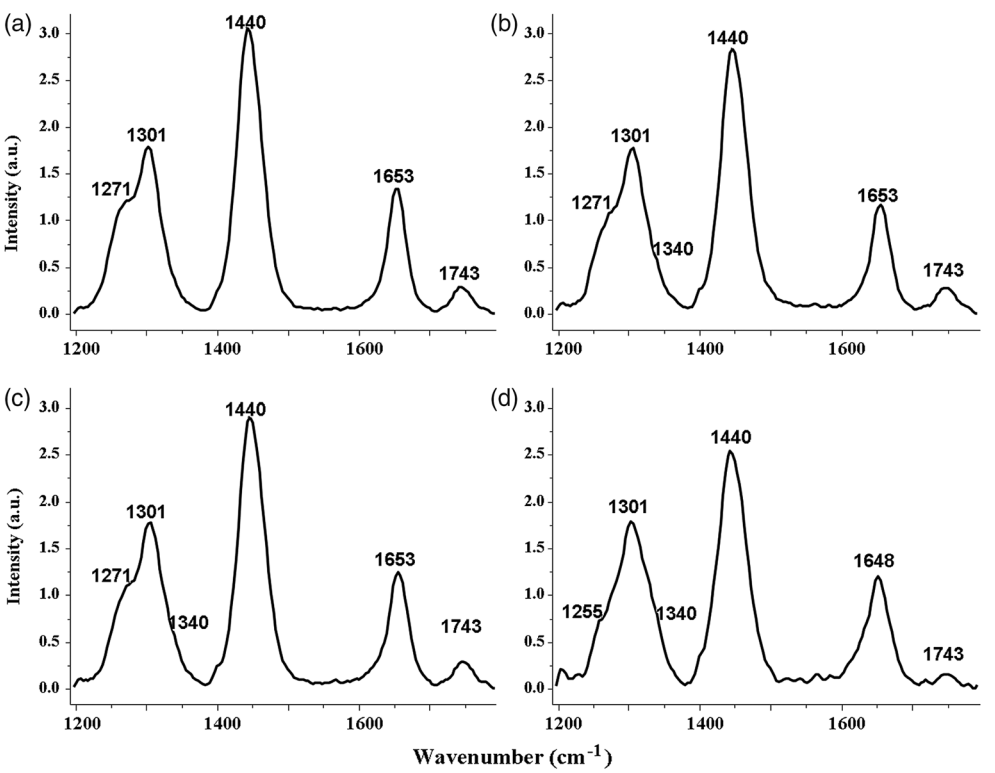

Fig. 2 Mean *in vivo* Raman spectra of breast from nonpregnant (a), pregnant (b), lactating (c), and tumor-bearing (d) mice interpolated in 1200 to 1800 cm^{-1} range.

difference spectra. Standard deviation was also calculated to illustrate intragroup variability (Fig. 3).

3 Results and Discussion

RS is sensitive to biochemical changes which, apart from detecting malignancy-associated changes in a breast, may also detect normal physiological changes that affect the breast. To establish the validity of this technique as a diagnostic tool, a study of confounding variables is important. Pregnancy/lactation, a process that induces massive changes in the breast, is one of the confounding factors. In this study, the sensitivity of RS to differentiate breasts of normal, pregnant, and lactating mice and its effect on the diagnosis of breast cancer was evaluated. The role of pregnancy and lactation in breast cancers has been extensively explored in mouse models.[23,24] Thus, a mouse model was used in the study. Moreover, such studies are difficult in human subjects; hence animal models are preferred.

3.1 *Spectral Analysis*

The spectral features of the mean control breast spectrum [Fig. 2(a)] 1743 cm^{-1} ($C=O$ ester); 1653 cm^{-1} (amide I); 1440 cm^{-1} (δ CH2); 1301 cm^{-1} (τ CH2); and 1271 cm^{-1} (amide III) can be attributed to lipids. Broad amide I, a change in features in the 1200 to 1400 cm^{-1} region of the mean tumor spectrum [Fig. 2(d)], suggests the dominance of proteins and DNA. A normal breast consists of mammary epithelium supported by a mammary fat pad rich in lipids, whereas a tumor is characterized by changes in protein profiles, an increase in cell proliferation, and changes in breast architecture. This explains lipid dominance in the control and variation in protein, increase in DNA, and loss of lipids in the tumors. These findings corroborate well with earlier studies.[6,7,25] The mean spectra of pregnancy and lactating breasts [Fig. 2(b) and 2(c), respectively] exhibit subtle but significant variations in the 1340 cm^{-1} region.

There are several methods to study the spectral variations among groups; independent component analysis,[6] curve deconvulation,[7] and difference spectrum[26] are amongst the widely used. In our study, difference spectrum was computed by subtracting mean control spectrum from mean pregnancy, lactation, and tumor spectra, respectively [Fig. 4(a1) through 4(a3)]. The negative peaks are due to the control spectrum and the positive peaks are due to pregnancy, lactation, or tumor spectra. The difference pregnancy spectrum [Fig. 4(a2)] shows the following changes: a loss of lipids (1268 cm^{-1}, 1743 cm^{-1}), an increase in DNA (1480 cm^{-1}, 1340 cm^{-1}), and an increase in proteins (1671 cm^{-1}, 1471 cm^{-1}, 1315 cm^{-1}). The difference lactating spectrum [Fig. 4(a2)] shows similar spectral features. Increase in proteins and DNA with a decrease in lipids may be attributed to an increase in the number of cell nuclei (cell division), which is known to take place during pregnancy and lactation. Tumor difference spectra [Fig. 4(a3)] suggests an increase in proteins (1671 cm^{-1}, 1456 cm^{-1}, 1471 cm^{-1}), an increase in DNA (1480 cm^{-1}, 1340 cm^{-1}), and a decrease in lipids (1743 cm^{-1}, 1440 cm^{-1}), which corroborates previous reports.[6,7] Changes in lipids and DNA suggest cell division, which is hallmark of tumorogenesis.[11] Some positive bands (1630 cm^{-1} and 1570 cm^{-1}) may be ascribed to blood.[27]

To understand the difference between pathological and physiological conditions, mean pregnancy and mean lactating

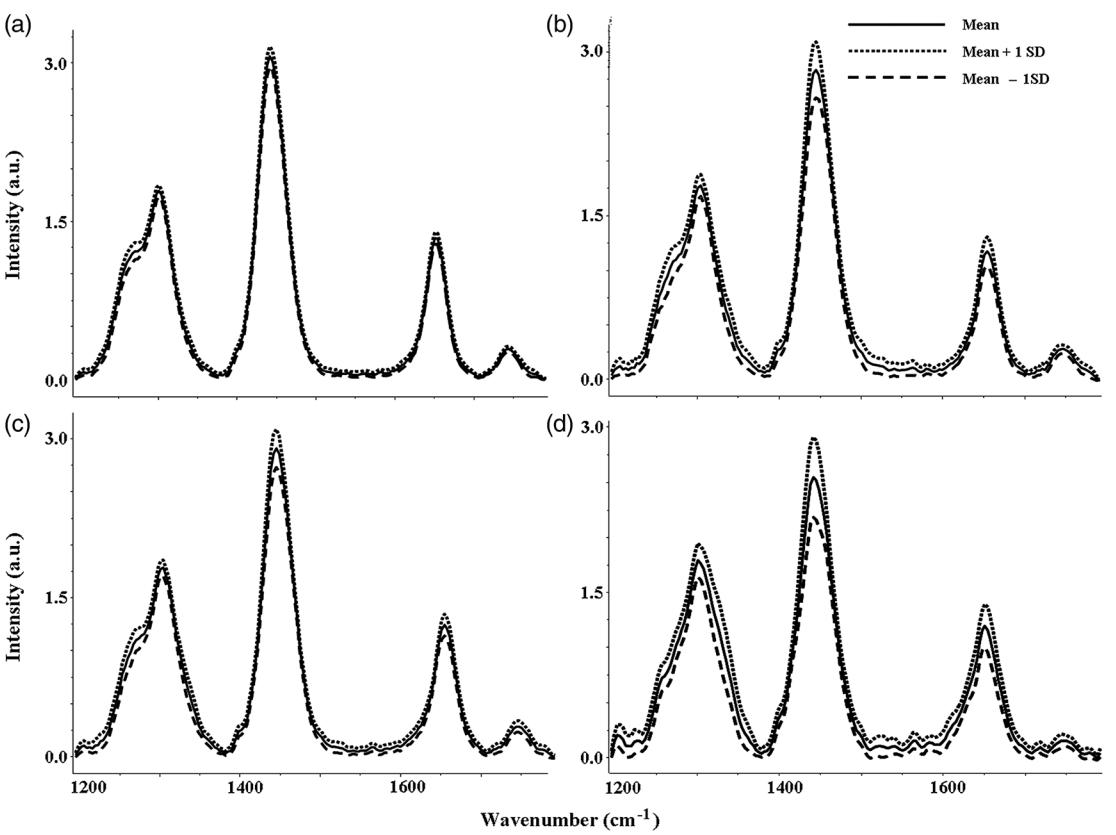

Fig. 3 Mean and standard deviation of transcutaneously recorded breast spectra from nonpregnant (a), pregnant (b), lactating (c), and tumor-bearing (d) mice interpolated in 1200 to 1800 cm^{-1} range.

spectrum were subtracted (individually) from the mean tumor spectrum. In this case, the positive bands are due to tumors and the negative bands due to pregnancy or lactation. The difference pregnancy (tumor – pregnancy) and the difference lactation (tumor – lactation) spectrum, shown in Fig. 4(b1) and 4(b2), suggests decrease in lipids (1743 cm^{-1}, 1440 cm^{-1}, and 1268 cm^{-1}) and an increase in DNA (1340 cm^{-1}) in tumors with respect to pregnancy or lactating conditions. Positive bands 1630 cm^{-1} and 1570 cm^{-1} may be ascribed to blood. Difference in the physiological spectrum [Fig. 4(c)] was also computed by subtracting the mean pregnancy spectrum from the mean lactating spectrum, wherein positive peaks are due to lactation and negative peaks due to pregnancy. In this case, the difference spectrum is very weak with respect to other difference spectra described above. Features 1450 cm^{-1} and 1660 cm^{-1} might indicate an increase in proteins in lactation with respect to pregnancy. The spectral assignments are based on available literature.[27]

3.2 *Classification of Pregnancy- and Lactation-Associated Changes*

To explore the feasibility of differentiating pregnant and lactating conditions from control, PC-LDA was used. Spectra interpolated in the 1200 to 1800 cm^{-1} range were used for analysis (several ranges were explored for the study, best classification was obtained in the mentioned range). To avoid overfitting, nine factors[28] contributing 86% of correct classifications were used [Fig. 5(a)]. The three-dimensional (3-D) plot of PC-LDA factors 1, 2, and 3 [Fig. 5(b)] suggests classification of nonpregnant (control) mice breasts from pregnant and lactating mice breasts, while the breast spectra of pregnant mice and lactating mice overlap.

The confusion matrix for the PC-LDA model building is shown in Table 1(a). In this analysis, 61 out of 61 spectra are correctly classified as control. Thirty-eight out of 56 spectra are correctly classified as pregnant breast condition, whereas 4 out of 56 are misclassified as control and 14 out of 56 are misclassified as lactating condition. Fifty-four of 59 spectra are correctly classified as lactating condition, whereas 5 of 59 are misclassified as pregnancy condition. LOOCV was carried out to evaluate the results obtained by LDA. LOOCV builds a model based on all observations but one and tests the left out observation against the model built; this is repeated until all observations are left out once. The performance is estimated in terms of classification efficiency, which is the percentage of spectra from each group that are correctly classified. In analysis of LOOCV as shown in Table 2(b), once again, 61 out of 61 spectra were correctly classified as control. Thirty-four of 56 spectra are correctly classified as pregnant breast condition, whereas 4 of 56

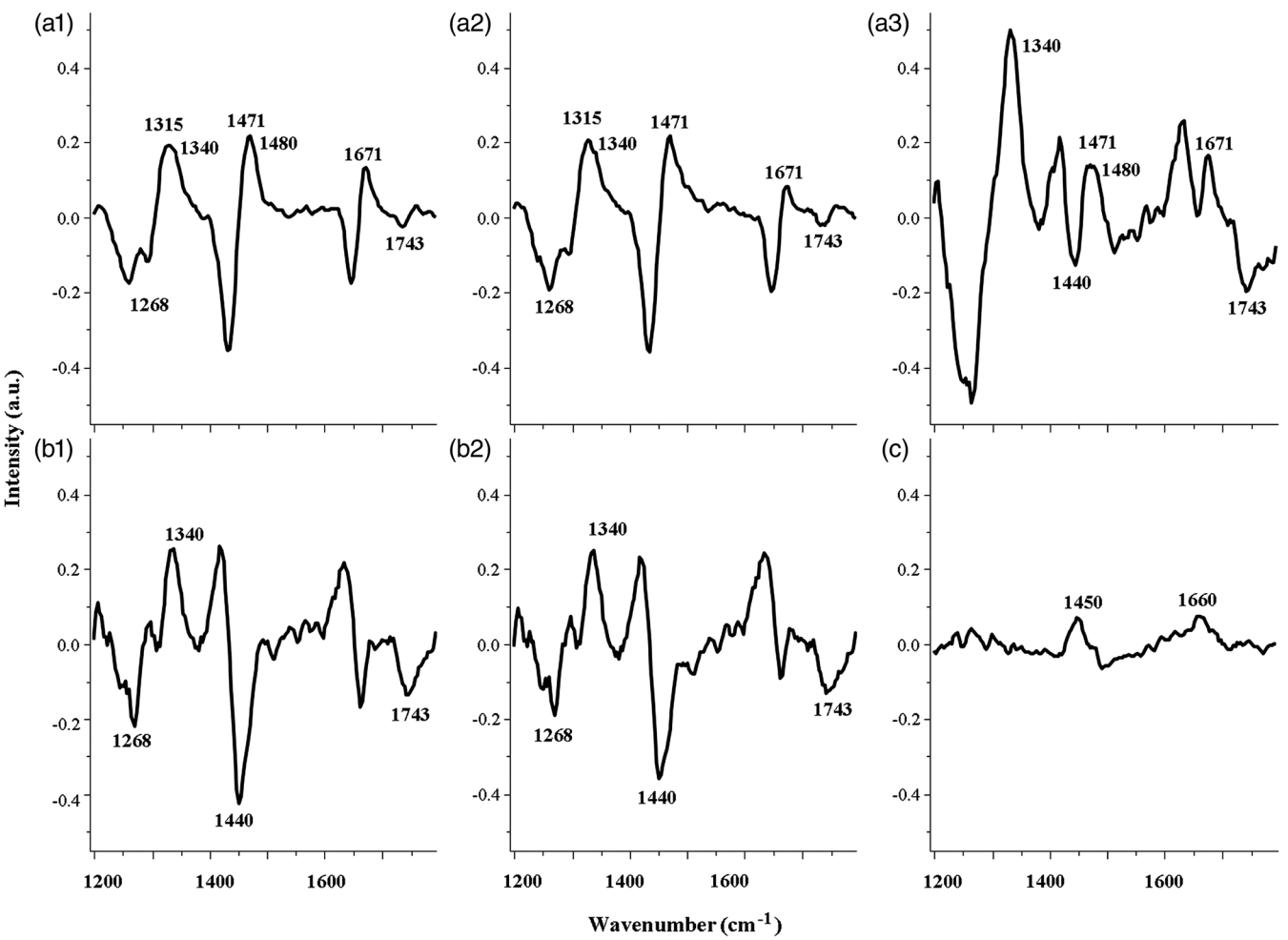

Fig. 4 Difference spectrum; pregnancy – control (a1); lactation – control (a2); tumor – control (a3); tumor – pregnancy (b1); tumor – lactation (b2); lactation – pregnancy (c).

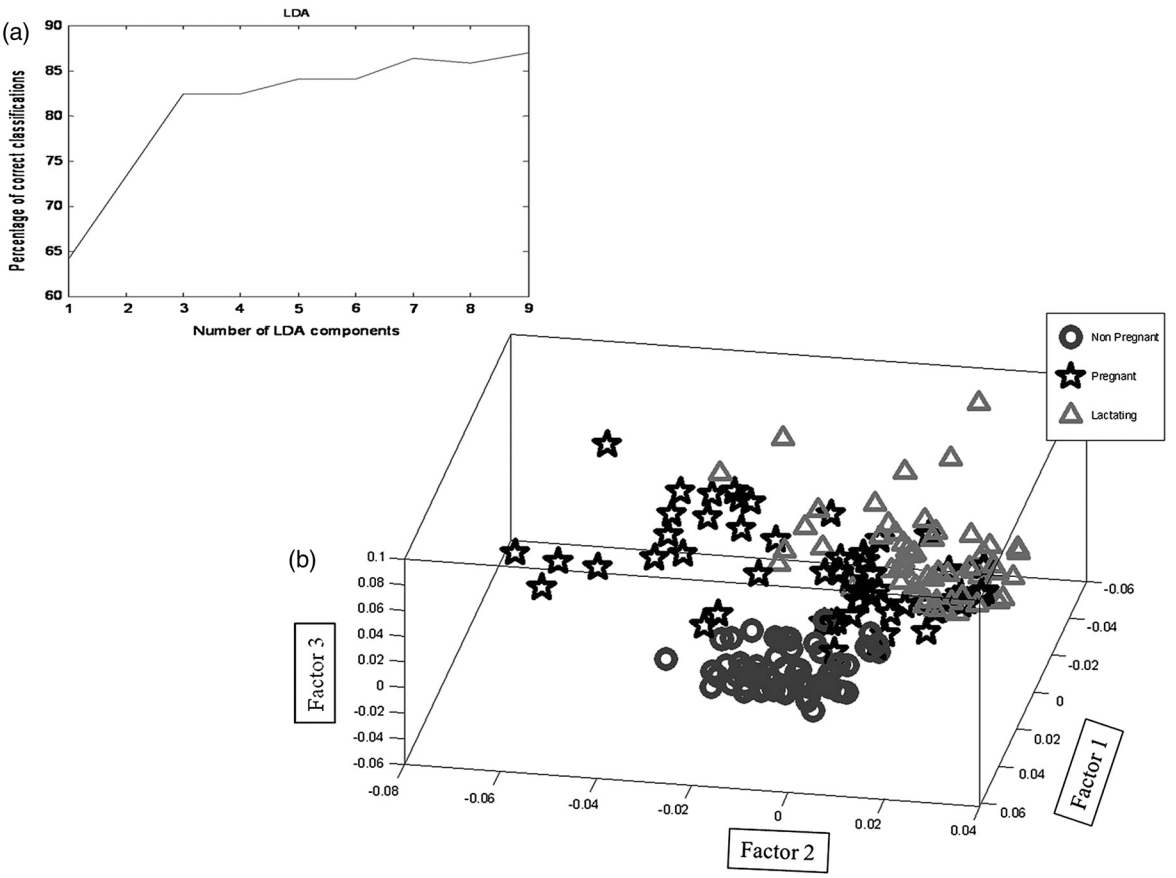

Fig. 5 PC-LDA to explore differences in mouse breast of nonpregnant, pregnant, and lactating mice: Scree plot (a) and 3-D plot of PC-LDA factors 1, 2, and 3 (b) suggesting classification between different breast conditions.

were misclassified as control and 18 of 56 were misclassified as lactating condition. As mentioned earlier, pregnancy is a phase midway between normal and lactation. This probably explains few misclassifications with normal breast. Both pregnant and lactation phases represent changes in breast as a result of rapid cell proliferation. This may explain high misclassification observed between pregnant and lactating conditions. Fifty-two of 59 spectra are correctly classified as lactating condition, while 7 of 59 were misclassified as pregnancy condition. The classification efficiency of lactation is higher than for pregnancy probably because lactation is characterized by cell differentiation and milk secretion in addition to cell proliferation. The classification efficiency of control, pregnant, and lactating mice breasts was 100%, 61%, and 88%, respectively.

It is important to note that several changes take place in breast skin during pregnancy and lactation. In humans, skin

Table 1 Confusion matrix for leave-one-out cross-validation of nonpregnant, pregnant, and lactating mouse breast: model building (a) and LOOCV (b) (diagonal elements are true positive predictions and ex-diagonal elements are false positive predictions). Sample size is shown in brackets.

Condition (no. of spectra, no. of animals used)	Nonpregnant	Pregnant	Lactating	Classification efficiency (%)
(a)				
Nonpregnant (61, 6)	61	0	0	100
Pregnant (56, 6)	4	38	14	68
Lactating (59, 6)	0	5	54	92
(b)				
Nonpregnant (61, 6)	61	0	0	100
Pregnant (56, 6)	4	34	18	61
Lactating (59, 6)	0	7	52	88

Table 2 Confusion matrix for leave-one-out cross-validation of nonpregnant, pregnant, lactating mouse breast, and frank breast tumors: model building (a) and LOOCV (b) (diagonal elements are true positive predictions and ex-diagonal elements are false positive predictions). Sample size is shown in brackets.

Condition (no. of spectra, no. of animals used)	Nonpregnant	Pregnant	Lactating	Frank breast tumors	Classification efficiency (%)
(a)					
Nonpregnant (61, 6)	61	0	0	0	100
Pregnant (56, 6)	4	35	17	0	63
Lactating (59, 6)	0	16	43	0	73
Frank breast tumors (40, 2)	1	0	0	39	98
(b)					
Nonpregnant (61, 6)	61	0	0	0	100
Pregnant (56, 6)	4	34	18	0	61
Lactating (59, 6)	0	18	41	0	69
Frank breast tumors (40, 2)	1	0	0	39	98

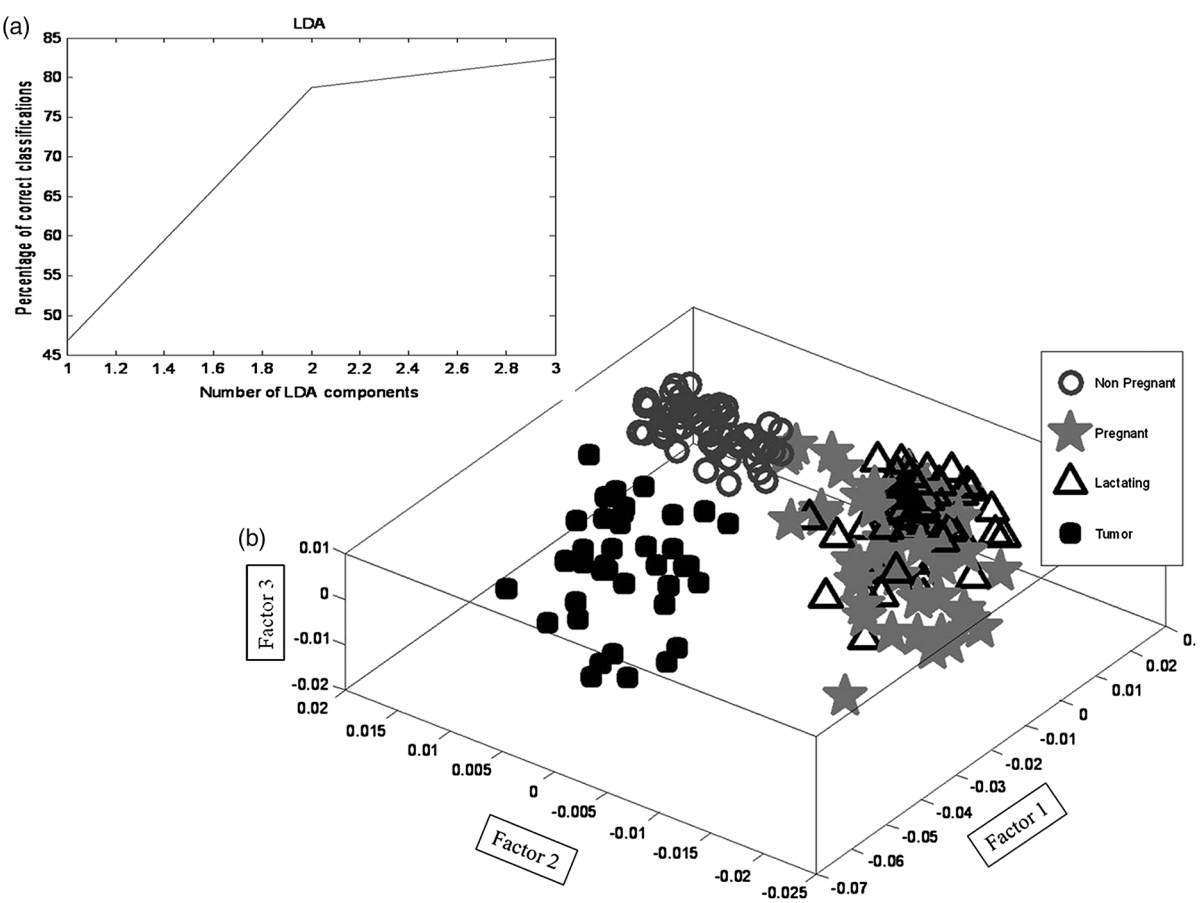

Fig. 6 PC-LDA to explore differences between breast spectra of tumor-bearing, nonpregnant, pregnant, and lactating mice: Scree plot (a) and 3-D plot of PC-LDA factors 1, 2, and 3 (b) suggesting classification between different breast conditions and frank breast tumors.

pigmentation increases, striae appear on breast skin, and skin gland secretions increase. Circulation to the skin increases and veins in the breast become more visible.[29] Thus, there is a possibility that these changes may affect breast spectra. In the present study, since a hairless variant of Swiss albino mice which lack pigments were used, pigmentation is not a factor. No striae appearance was observed. With respect to blood flow and vascularization, in this study, no spectral bands attributable to blood were observed. Tumor development involves angiogenesis (increased blood vessels and blood flow), but spectral features of blood have not been reported in transcutaneous spectra of breast tumors.[30] However, in the difference spectrum of current study—tumor – control, tumor – pregnancy, and tumor – lactation—some bands may be ascribed to blood.

3.3 *Classification of Frank Breast Tumors from Pregnancy/Lactation*

The possibility of classifying frank tumors from pregnancy- or lactation-associated changes was explored using PC-LDA. For analysis, three factors contributing to 82% of correct classifications were used [Fig. 6(a)]. The 3-D plot of PC-LDA factors 1, 2, and 3 [Fig. 6(b)] suggests classification of frank tumors from normal, pregnant, and lactating mice. The confusion matrices for model building and LOOCV are shown in Tables 2(a) and 2(b), respectively. Sixty-one out of 61 spectra are correctly classified as control, whereas 34 out of 56 and 41 out of 59, respectively, are correctly classified as pregnancy and lactation. Four out of 56 pregnancy spectra were misclassified as control, while 18 out of 59 were misclassified as lactating. No misclassification with respect to tumors was observed. Eighteen out of 59 of lactation misclassified with pregnancy, whereas no misclassifications with control or tumor are observed. These results mirror previous observations (Sec. 3.2). Since pregnancy is a phase between control and lactation, misclassifications with both were observed. Pregnancy and lactation are both characterized by cell proliferation, hence the observed misclassifications amongst them.

Thirty-nine out of 40 tumor spectra classify correctly as tumor. Only 1 of 40 misclassified as control. It is known that tumors are a heterogeneous complex of necrotic centers, rapidly proliferating fronts, and normal patches. This probably explains misclassification with normal breast. The classification efficiency of frank tumors from pregnancy/lactation conditions is 97.5%. Results suggest minimal effect of pregnancy- and lactation-associated changes on detection of frank tumors using RS.

4 Conclusion

RS is a rapid, objective, and potentially noninvasive technique that can provide a "molecular fingerprint" of a sample. Hence, it has been extensively explored as a potential diagnostic tool for breast cancer. However, normal physiological changes like pregnancy and/or lactation affect the biochemical composition of the breast. To establish the validity of any diagnostic tool, a study of such confounding variables is important. In this study, the ability of this technique to identify pregnancy- and/or lactation-associated changes and its effect on tumor detection was evaluated. Results suggest that this technique can identify the above changes. Further, these physiological changes do not affect ability of RS to detect tumors. Further studies with precancerous and benign conditions are warranted.

References

1. A. Jemal et al., "Global cancer statistics," *CA Cancer J. Clin.* **61**(2), 69–90 (2011).
2. N. Howlader et al., Ed., *SEER Cancer Statistics Review, 1975–2008 (Vintage 2009 Populations)*, National Cancer Institute, Bethesda, Maryland (2011), http://seer.cancer.gov/csr/1975_2009_pops09/.
3. S. M. Ismail et al., "Observer variation in histopathological diagnosis and grading of cervical intraepithelial neoplasia," *Br. Med. J.* **298**(6675), 707–710 (1989).
4. J. B. Sorensen et al., "Interobserver variability in histopathologic subtyping and grading of pulmonary adenocarcinoma," *Cancer* **71**(10), 2971–2976 (1993).
5. D. J. Evers et al., "Optical spectroscopy: current advances and future applications in cancer diagnostics and therapy," *Future Oncol.* **8**(3), 307–320 (2012).
6. S. Haka et al., "Diagnosing breast cancer by using Raman spectroscopy," *Proc. Natl. Acad. Sci. U.S.A.* **102**(35), 12371–12376 (2005).
7. M. V. P. Chowdary et al., "Biochemical correlation of Raman spectra of normal, benign and malignant breast tissues: a spectral deconvolution study," *Biopolymers* **91**(7), 539–546 (2009).
8. C. V. Raman and K. S. Krishnan, "A new type of secondary radiation," *Nature* **121**(3048), 501–502 (1928).
9. S. R. Oakes, H. N. Hilton, and C. J. Ormandy, "Key stages in mammary gland development—The alveolar switch: coordinating the proliferative cues and cell fate decisions that drive the formation of lobuloalveoli from ductal epithelium," *Breast Cancer Res.* **8**(207), 1–10 (2006).
10. M. M. Richert et al., "An atlas of mouse mammary gland development," *J. Mammary Gland Biol.* **5**(2), 227–241 (2000).
11. B. S. Wiseman and Z. Werb, "Stromal effects on mammary gland development and breast cancer," *Science* **296**(5570), 1046–1049 (2002).
12. V. Djonov, A. C. Andres, and A. Ziemiecki, "Vascular remodelling during the normal and malignant life cycle of the mammary gland," *Microsc. Res. Tech.* **52**(2), 182–189 (2001).
13. R. A. Bhisey, P. L. Veturkar, and A. Borges, "Comparison of sensitivity of Swiss albino and hairless Swiss bare mice to two stage skin tumorigenesis," *Indian J. Exp. Biol.* **25**(2), 90–96 (1987).
14. S. R. Pai and P. G. Save, " Influence of high dose of estradiol on ICRC mouse bearing transplanted mammary tumours," *Indian J. Med. Res.* **64**(12), 1788–1789 (1976).
15. S. P. Singh et al., "Raman spectroscopy in head and neck cancers: towards oncological applications," *J. Cancer Res. Ther.* **8**(6), S126–S132 (2012).
16. A. Sahu et al., "Raman spectroscopy of oral buccal mucosa: a study on age-related physiological changes and tobacco-related pathological changes," *Technol. Cancer Res. Treat.* **11**(6), 528–623 (2012).
17. A. Nijssen et al., "Discriminating basal cell carcinoma from perilesional skin using high wave-number Raman spectroscopy," *J. Biomed. Opt.* **12**(3), 034004 (2007).
18. S. Koljenovic et al., "Discriminating vital tumor from necrotic tissue in human glioblastoma tissue samples by Raman spectroscopy," *Lab. Invest.* **82**(10), 1265–1277 (2002).
19. C. Kendall et al., "Evaluation of Raman probe for oesophageal cancer diagnostics," *Analyst* **135**(12), 3038–3041 (2010).
20. T. J. Harvey et al., "Factors influencing the discrimination and classification of prostate cancer cell lines by FTIR microspectroscopy," *Analyst* **134**(6), 1083–1091 (2009).
21. A. Ghanate et al., "Comparative evaluation of spectroscopic models using different multivariate statistical tools in a multicancer scenario," *J. Biomed. Opt.* **16**(2), 025003 (2011).
22. S. Balakrishnama and A. Ganapathiraju, "Linear discriminant analysis—A brief tutorial," (1998), http://lcv.stat.fsu.edu/research/geometrical_representations_of_faces/PAPERS/lda_theory.pdf.
23. D. Medina, "Mammary developmental fate and breast cancer risk," *Endocr. Relat. Cancer* **12**(3), 483–495 (2005).
24. J. Russo et al., "The protective role of pregnancy in breast cancer," *Breast Cancer Res.* **7**(3), 131–142 (2005).
25. R. E. Kast et al., "Raman spectroscopy can differentiate malignant tumors from normal breast tissue and detect early neoplastic changes in a mouse model," *Biopolymers* **89**(3), 235–241 (2008).
26. M. V. Chowdary et al., "Discrimination of normal, benign, and malignant breast tissues by Raman spectroscopy," *Biopolymers* **83**(5), 556–569 (2006).

27. F. S. Parker, *Application of Infrared, Raman, and Resonance Raman spectroscopy in Biochemistry*, Plenum Press, New York (1983).
28. J. Kelly et al., "Biospectroscopy to metabolically profile biomolecular structure: a multistage approach linking computational analysis with biomarkers," *J. Proteome Res.* **10**(4), 1437–1448 (2011).
29. C. Schaefer and P. Peters, "Dermatological medicine and local therapeutics," Chapter 2.10 in *Drugs During Pregnancy and Lactation*, C. Schaefer, Ed., pp. 105–106, Elsevier Science, Amsterdam, The Netherlands (2001).
30. L. Raniero et al., "In and *ex vivo* breast disease study by Raman spectroscopy," *Theor. Chem. Acc.* **130**(4–6), 1239–1247 (2011).